Quantum Chromodynamics

lecture IV

Sven-Olaf Moch

Universität Hamburg

IMSc Spring School on High Energy Physics

Chennai, Feb 27, 2025

Plan

- Introduction to QCD
  Monday, February 24, 2025
- QCD at work: infrared safety and jets
  Tuesday, February 25, 2025
- QCD at work: factorization and evolution
  Wednesday, February 26, 2025
- *Deep structure of proton*
  Thursday, February 27, 2025

QCD evolution

- Evolution formulates dependence of cross sections for observable on momentum transfer
- Classic example: scaling violations of structure functions
  Gross, Wilczek '73; Politzer '73
- Physical cross section in factorization ansatz cannot depend on μ
  $Q^2\, \sigma_{\rm phys}\,(Q) = \hat{\sigma}_{\rm pt}\,(Q/\mu, \alpha_s(\mu)) \,\otimes\, f\,(\mu)$
  - factorization scale μ arbitrary $\mu \frac{d\,\sigma_{\rm phys}}{d\mu} = 0$
- Immediate consequence parton evolution   Altarelli, Parisi '77

$$\mu \frac{d\,f(\mu)}{d\mu} = P\,(\alpha_s(\mu)) \,\otimes\, f(\mu) + \mathcal{O}\left(\frac{1}{Q^2}\right)$$

$$\mu \frac{d\,\hat{\sigma}_{\rm pt}\,(Q/\mu, \alpha_s(\mu))}{d\mu} = -P\,(\alpha_s(\mu)) \,\otimes\, \hat{\sigma}_{\rm pt}\,(Q/\mu, \alpha_s(\mu)) + \mathcal{O}\left(\frac{1}{Q^2}\right)$$

- PDF evolution from renormalization group equation

QCD evolution

- Evolution formulates dependence of cross sections for observable on momentum transfer
- Classic example: scaling violations of structure functions
  Gross, Wilczek '73; Politzer '73
- Physical cross section in factorization ansatz cannot depend on μ
  $Q^2\,\sigma_{\rm phys}\,(Q) = \hat{\sigma}_{\rm pt}\,(Q/\mu, \alpha_s(\mu))\,\otimes\, f\,(\mu)$
  - factorization scale μ arbitrary $\mu \frac{d\,\sigma_{\rm phys}}{d\mu} = 0$
- Immediate consequence parton evolution Altarelli, Parisi '77

$$\mu \frac{d\,f(\mu)}{d\mu} = P\,(\alpha_s(\mu)) \otimes f(\mu) + \mathcal{O}\left(\frac{1}{Q^2}\right)$$

$$\mu \frac{d\,\hat{\sigma}_{\rm pt}\,(Q/\mu, \alpha_s(\mu))}{d\mu} = -P\,(\alpha_s(\mu)) \otimes \hat{\sigma}_{\rm pt}\,(Q/\mu, \alpha_s(\mu)) + \mathcal{O}\left(\frac{1}{Q^2}\right)$$

- PDF evolution from renormalization group equation
  - splitting functions calculable in QCD

Mass factorization

- NLO correction to Drell-Yan process
  - absorb collinear divergence $P_{qq}^{(0)}$ in renormalized parton distributions

$$\hat{\sigma}_{q\bar{q}\to V}^{(1),\mathrm{bare}}(x) \quad = \quad \frac{\alpha_s}{4\pi}\left(\frac{\mu^2}{M_V^2}\right)^{\epsilon}\left\{\frac{1}{\epsilon}\,2\,P_{qq}^{(0)}(x)+\hat{\sigma}_{q\bar{q}\to V}^{(1)}(x)+\mathcal{O}(\epsilon)\right\}$$

$$f_q^{p,\mathrm{ren}}(x,\mu_F^2) \quad = \quad f_q^{p,\mathrm{bare}}(x)-\frac{\alpha_s}{4\pi}\,\frac{1}{\epsilon}\left(\frac{\mu^2}{\mu_F^2}\right)^{\epsilon}\left[P_{qq}^{(0)}(x)\otimes f_q^{p,\mathrm{bare}}\right](x)$$

QCD evolution

- Scale evolution of parton distributions
  - use $\dfrac{d}{d\ln\mu_F^2}f_q^{p,\mathrm{bare}}(x)=0$ to derive QCD evolution equation

$$\frac{d}{d\ln\mu_F^2}f_q^{p,\mathrm{ren}}(x,\mu_F^2) \quad = \quad \left[P_{qq}^{(0)}(x)\otimes f_q^{p,\mathrm{ren}}\right](x,\mu_F^2)$$

Parton evolution

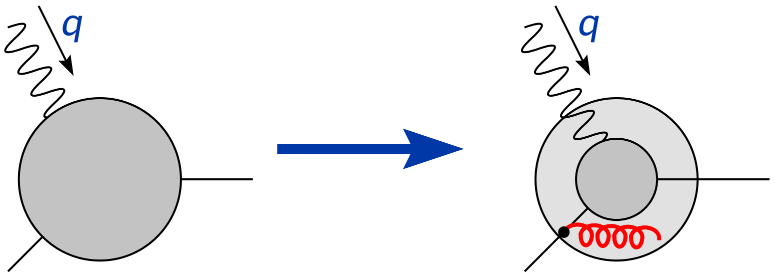

- Feynman diagrams in leading order

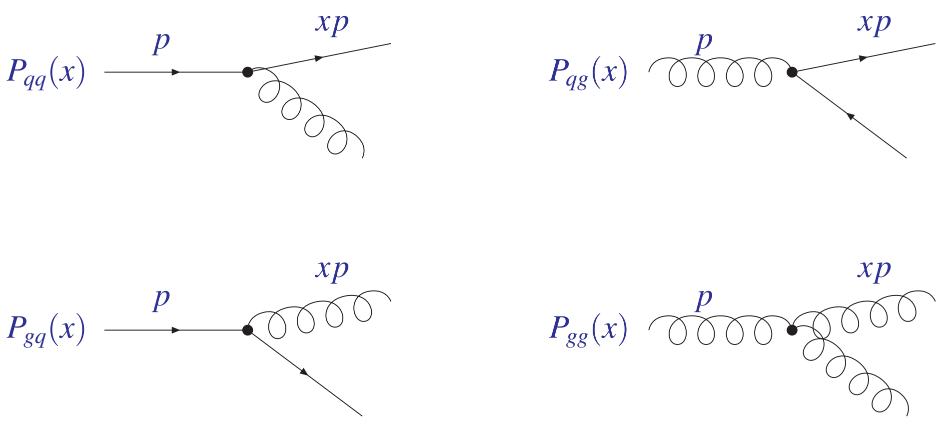

- Proton in resolution $1/Q \longrightarrow$ sensitive to lower momentum partons
- Evolution equations for parton distributions f_i
  - predictions from fits to reference processes (universality)

$$\frac{d}{d\ln\mu^2} f_i(x,\mu^2) = \sum_k \left[P_{ik}(\alpha_s(\mu^2)) \otimes f_k(\mu^2) \right](x)$$

- Splitting functions P up to N^{3}LO (work in progress)

$$P = \underbrace{\alpha_s P^{(0)} + \alpha_s^2 P^{(1)} + \alpha_s^3 P^{(2)}}_{\text{NNLO: standard approximation}} + \alpha_s^4 P^{(3)} + \ldots$$

Complete set of splitting functions and PDFs

- Evolution equations
  - non-singlet ($2n_f - 1$ scalar) and singlet (2×2 matrix) equations

$$\frac{d}{d\ln\mu^2} f_i(x,\mu^2) \;=\; \sum_k \left[P_{ik}(\alpha_s(\mu^2)) \otimes f_k(\mu^2)\right](x)$$

Complete set of splitting functions and PDFs

- Evolution equations
  - non-singlet ($2n_f - 1$ scalar) and singlet (2×2 matrix) equations

$$\frac{d}{d \ln \mu^2} f_i(x, \mu^2) = \sum_k \left[P_{ik}(\alpha_s(\mu^2)) \otimes f_k(\mu^2) \right](x)$$

- Non-singlet and singlet distributions $q^{\pm}$, q^{v} and q_{s}, g

$$q^{\pm}_{\mathrm{ns},ik} = q_i \pm \bar{q}_i - (q_k \pm \bar{q}_k)$$

flavour asymmetries

$$q^{\mathrm{v}}_{\mathrm{ns}} = \sum_{r=1}^{n_f} (q_r - \bar{q}_r)$$

total valence distribution

$$q_{\mathrm{s}} = \sum_{r=1}^{n_f} (q_r + \bar{q}_r)$$

flavour singlet distribution, $f_i = \begin{pmatrix} q_{\mathrm{s}} \\ g \end{pmatrix}$

Complete set of splitting functions and PDFs

- Evolution equations
  - non-singlet ($2n_f - 1$ scalar) and singlet (2×2 matrix) equations

$$\frac{d}{d\ln\mu^2} f_i(x,\mu^2) \;=\; \sum_k \left[P_{ik}(\alpha_s(\mu^2)) \otimes f_k(\mu^2)\right](x)$$

- Non-singlet and singlet distributions $q^{\pm}$, $q^{\rm v}$ and $q_{\rm s}$, g

$$q^{\pm}_{{\rm ns},ik} \;=\; q_i \pm \bar{q}_i - (q_k \pm \bar{q}_k) \qquad \text{flavour asymmetries}$$

$$q^{\rm v}_{\rm ns} \;=\; \sum_{r=1}^{n_f} (q_r - \bar{q}_r) \qquad \text{total valence distribution}$$

$$q_{\rm s} \;=\; \sum_{r=1}^{n_f} (q_r + \bar{q}_r) \qquad \text{flavour singlet distribution,} \quad f_i = \begin{pmatrix} q_{\rm s} \\ g \end{pmatrix}$$

- Splitting function combinations

$$P^{\pm}_{\rm ns}\,, \qquad P^{\rm v}_{\rm ns} \;=\; P^{-}_{\rm ns} + P^{\rm s}_{\rm ns} \qquad \text{non-singlet}$$

$$P_{\rm s} = \begin{pmatrix} P_{\rm qq} & P_{\rm qg} \\ P_{\rm gq} & P_{\rm gg} \end{pmatrix}, \qquad P_{\rm qq} \;=\; P^{+}_{\rm ns} + P_{\rm ps} \qquad \text{singlet}$$

Parton distributions in proton

- Valence $q - \bar{q}$ (additive quantum numbers) sea (part with $q + \bar{q}$)

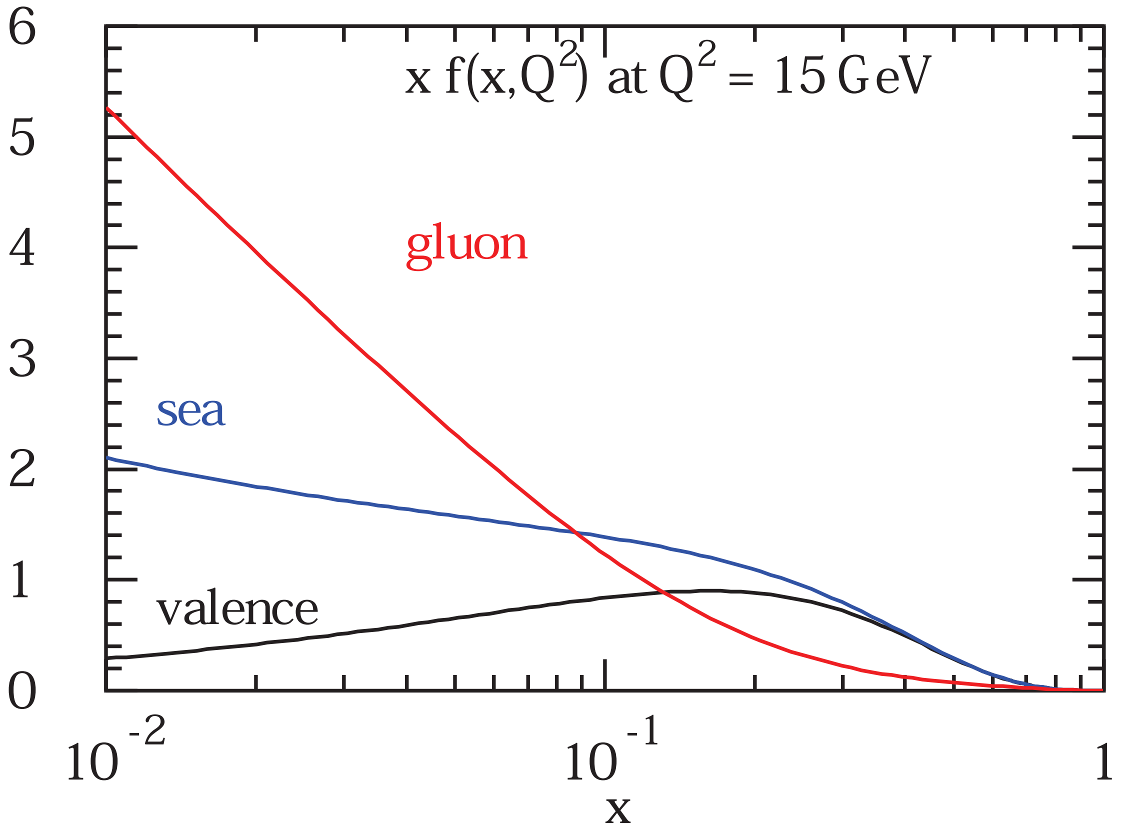

- Parameterization (bulk of data from deep-inelastic scattering)
  - structure function $F_2 \longrightarrow$ quark distribution
  - scale evolution (perturbative QCD) $\longrightarrow$ gluon distribution

Parton distributions in proton

- Valence $q - \bar{q}$ (additive quantum numbers) sea (part with $q + \bar{q}$)

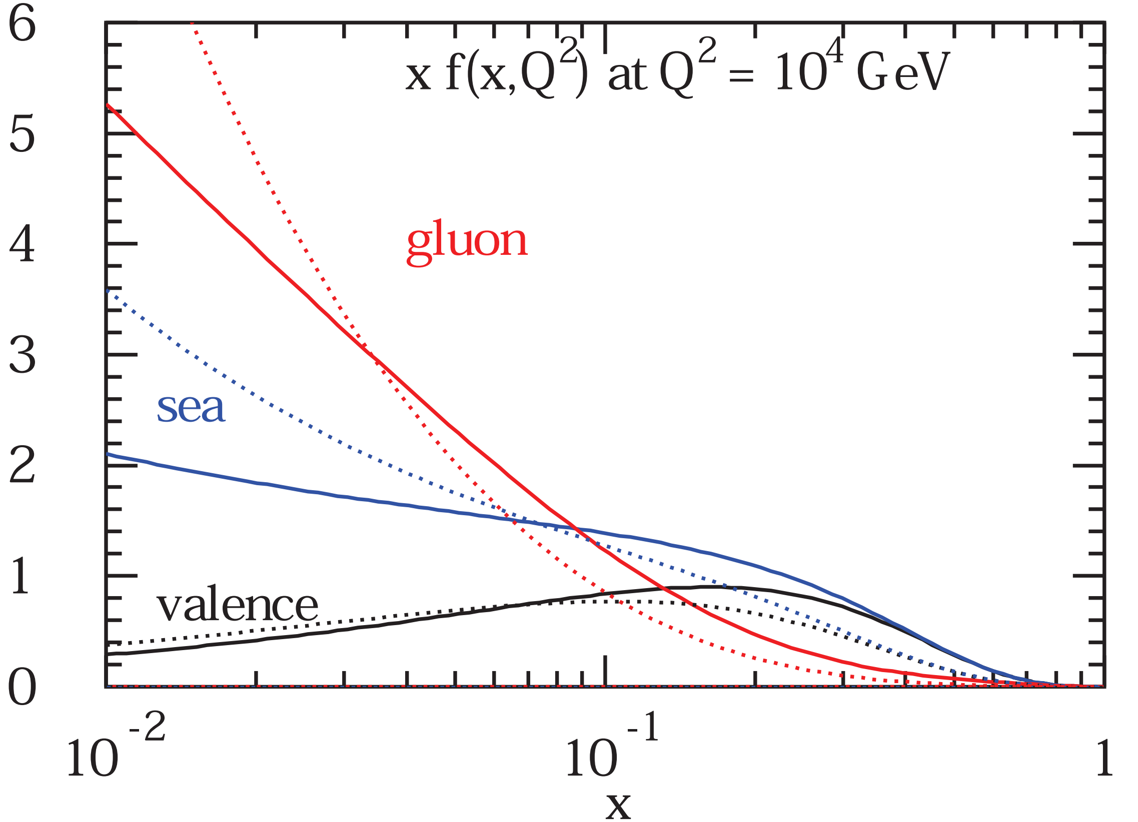

- Parameterization (bulk of data from deep-inelastic scattering)
  - structure function $F_2 \longrightarrow$ quark distribution
  - scale evolution (perturbative QCD) $\longrightarrow$ gluon distribution

Pocket partonometer

Volume 172, number 3,4 PHYSICS LETTERS B 22 May 1986

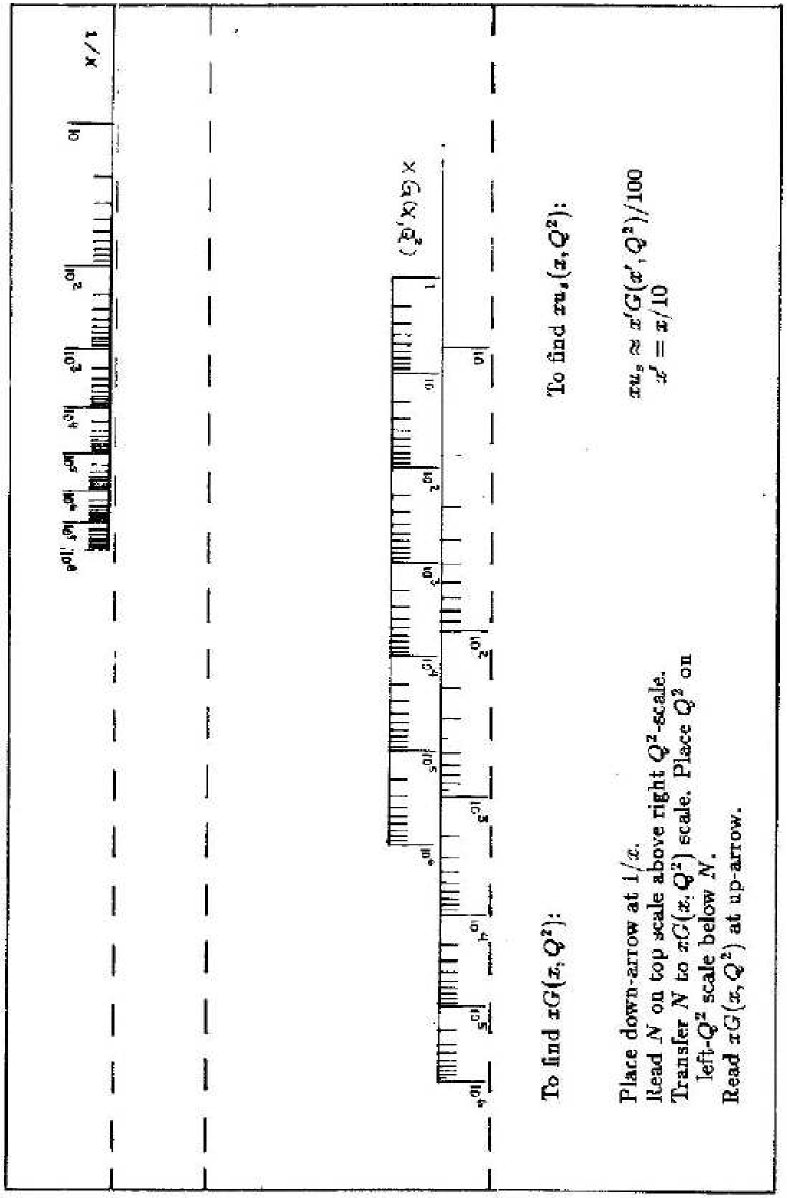

Volume 172, number 3,4 PHYSICS LETTERS B 22 May 1986

for t- or heavier particle distributions one must model thresholds numerically such as done in ref. [4] [‡3]. However, departures from a symmetrically distributed sea, which complicate the boundary conditions, can be reproduced by the ratios $u_s \approx d_s \approx s_s \approx 2c_s \approx 2b_s$.

The analytic gluon solution (3), boundary conditions included, is calculated by the partonometer (fig. 2). The scales automate the logarithms of certain functions of $1/x$ and Q^2 left to the reader. In systematic testing the accuracy of the gizmo is at the 10–20% level depending on the operator's ability to read logarithmic scales. It is much better than interpolating between graphs such as fig. 1a. The speed is even faster than adding a new card [‡4] to an existing program that runs.

Gluon distributions are read off directly; see the example below. Quark sea distributions can be evaluated using the identity

$$xu_s(x, Q^2) = (2/b)\partial xG(x, Q^2)/\partial y, \qquad (7)$$

and evaluating the derivative numerically. But wait! To minimize reading errors, one finds that the derivative above and the normalization change are roughly represented by

$$xu_s(x, Q^2) \approx x'G(x', Q^2)/100, \quad x' = x/10. \qquad (8)$$

This estimate is actually quite close to the re-scaled $xu_s(x, Q^2)$ of ref. [5] and is not too bad a match to

[‡4] Private communication with well known phenomenologist.

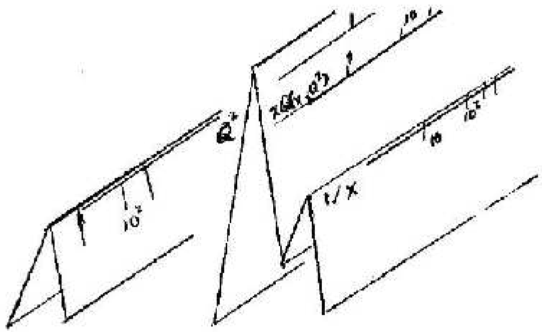

Fig. 2. The partonometer. To assemble: cut on solid lines, fold on dotted lines.

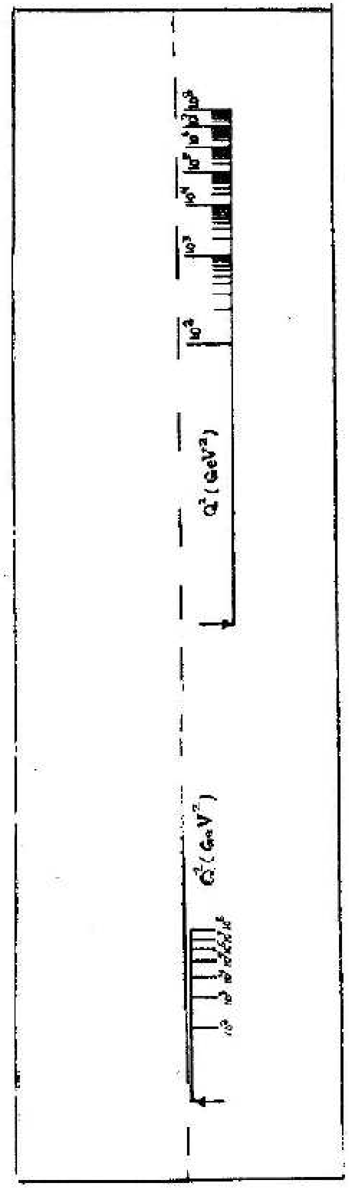

LHAPDF database

- Essential tool for implementation of parton distribution functions in wide range of analyses https://www.lhapdf.org/
- **Purpose:** Standardized access to PDFs for high-energy physics
- **Compatibility:** Supports various PDF sets from collaborations like ABMP, CTEQ, MSHT, NNPDF, etc
- **Interfacing:** Can be integrated with multiple event generators and numerical tools
- **Uncertainty Quantification:** Provides central values and uncertainty measures for PDFs
- **Versioning:** Regularly updated to include new PDF sets and improvements
- **Documentation:** Extensive guides and tutorials for users of all skill levels

Parton content of the proton

The LHC

- Highest energies at colliders until 203x

Parton kinematics at LHC

- Information on proton structure depends on kinematic coverage

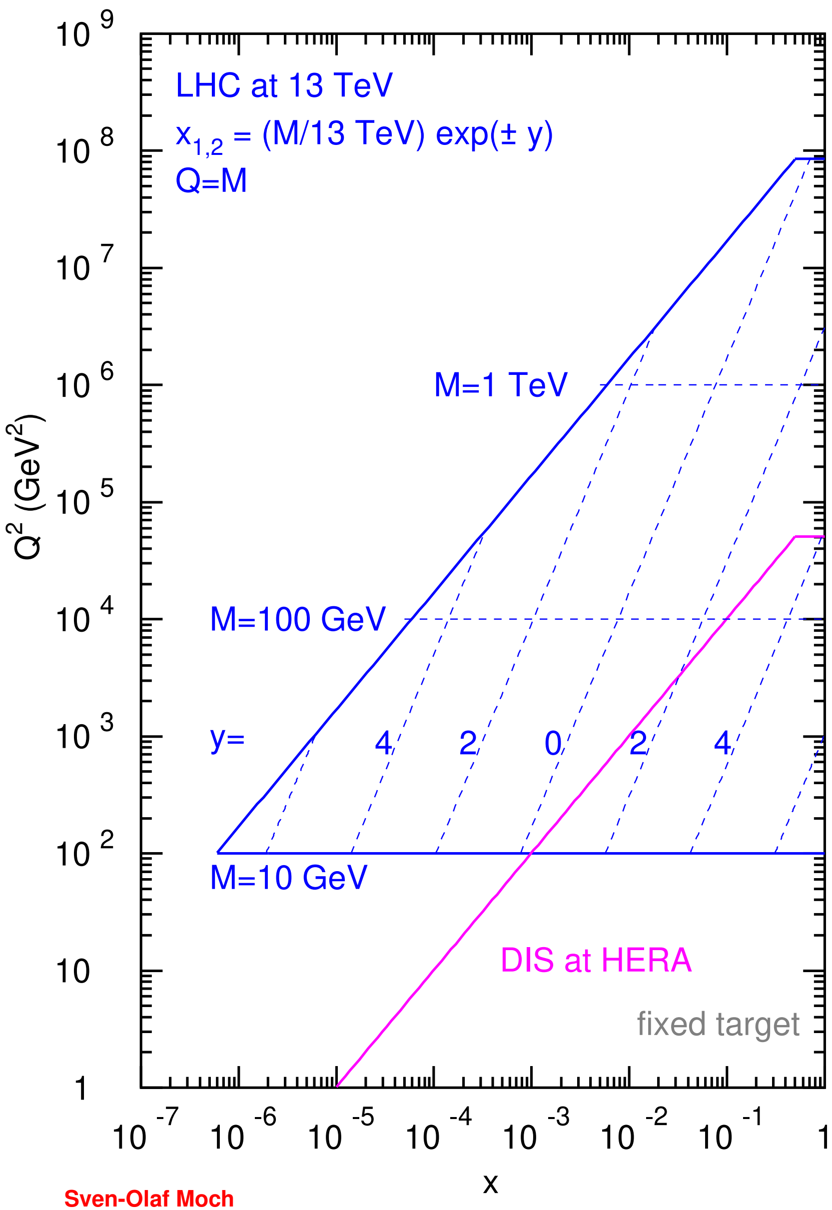

- LHC run at $\sqrt{s}$ = 13 TeV
  - parton kinematics well covered by HERA and fixed target experiments
- Parton kinematics with $x_{1,2} = M/\sqrt{S}\mathrm{e}^{\pm y}$
  - forward rapidities sensitive to small-x
- Cross section depends on convolution of parton distributions
  - small-x part of f_i and large-x PDFs f_j

$$\sigma_{pp\to X} = \sum_{ij} f_i(\mu^2) \otimes f_j(\mu^2) \otimes \left[\ldots \right]$$

Parton kinematics at EIC

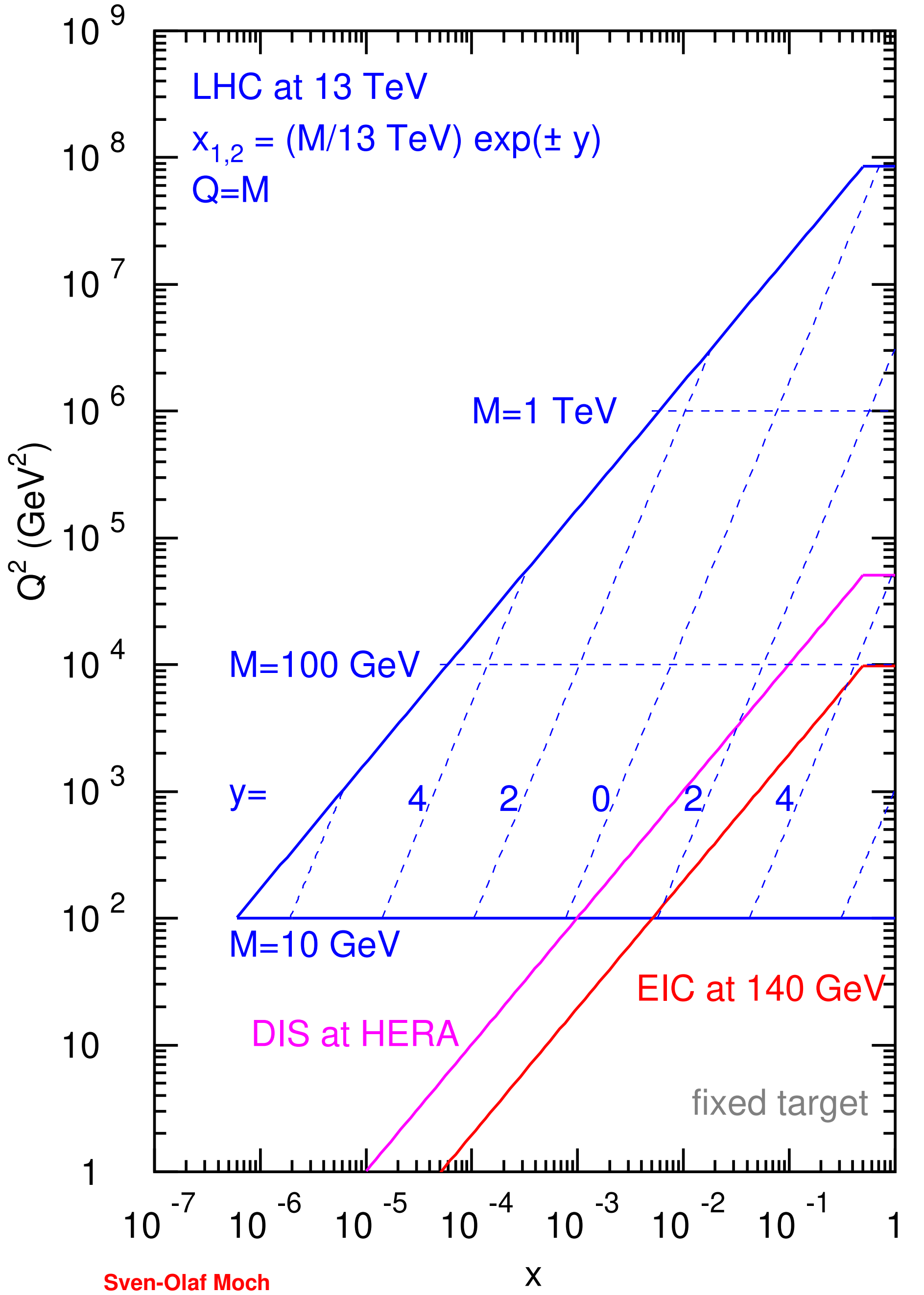

- EIC run at $\sqrt{s}$ = 140 GeV
  - ep-collisions at EIC cover large part of phase space relevant for LHC
  - overlap with HERA and fixed target experiments

Novel measurements at EIC

- 3D-images of hadron in position and momentum space (including spin)
- Measurements with unprecedented precision

Parton kinematics at LHeC

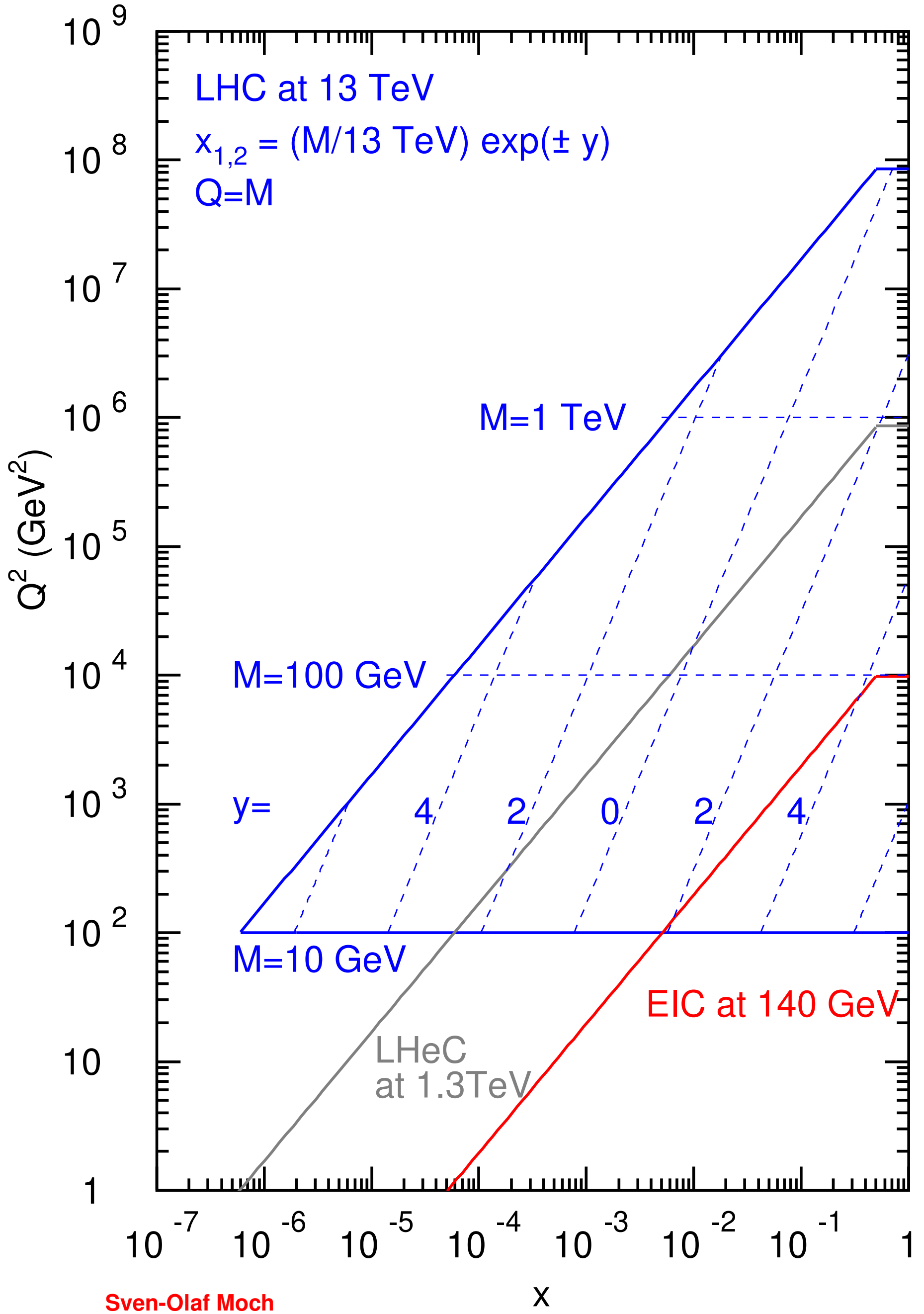

- LHeC run at $\sqrt{s}$ = 1.3 TeV
  - significant reach beyond HERA kinematics

New QCD regime accessible

- exploration of parton dynamics at small $x \simeq 10{-}6$

Parton kinematics at FCC-hh

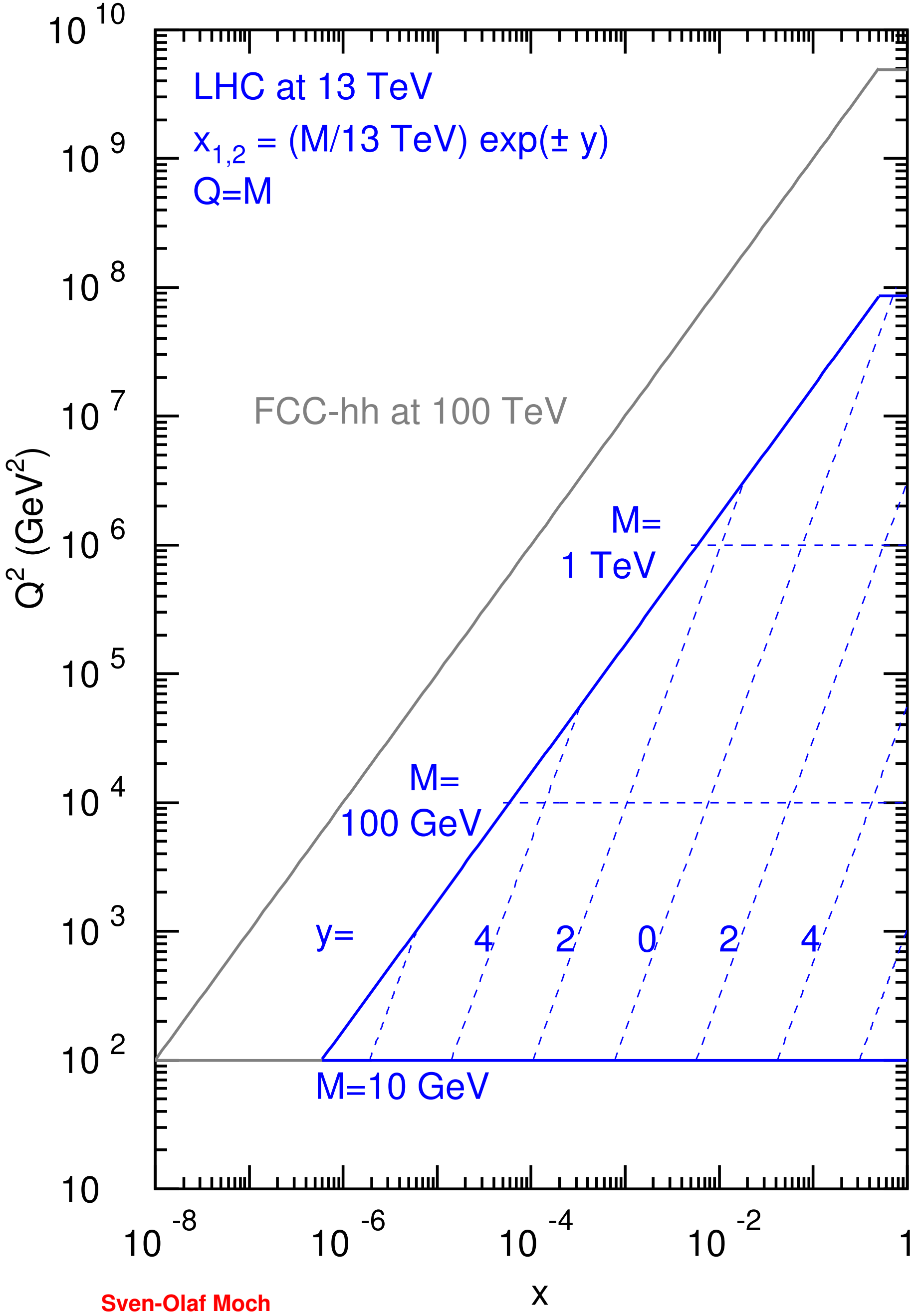

- FCC-hh run at $\sqrt{s}$ = 100 TeV
  - parton kinematics way beyond LHC
    Watch the scales on axes of plot!
- Significant sensitivity ot parton dynymics at small-x
  - low scales Q and forward rapidities probe $x \simeq 10^{-7}$
  - high scales $Q \simeq 10 \ldots 50$ TeV need PDFs at large $x \simeq 0.1 \ldots 0.8$

Data in global PDF fits

Data sets considered in ABMP16 analysis

Alekhin, Blümlein, S.M., Placakyte '17

- Analysis of world data for deep-inelastic scattering, fixed-target data for Drell-Yan process and collider data ($W^{\pm}$-, Z-bosons, top-quarks)
  - inclusive DIS data HERA, BCDMS, NMC, SLAC ($NDP = 2155$)
  - semi-inclusive DIS charm-, bottom-quark data HERA ($NDP = 81$)
  - Drell-Yan data (fixed target) E-605, E-866 ($NDP = 158$)
  - neutrino-nucleon DIS (di-muon data) CCFR/NuTeV, CHORUS, NOMAD ($NDP = 232$)
  - $W^{\pm}$-, Z-boson production data D0, ATLAS, CMS, LHCb ($NDP = 172$)
  - inclusive top-quark hadro-production CDF&D0, ATLAS, CMS ($NDP = 24$)

Iterative cycle of PDF fits

i) check of compatibility of new data set with available world data

ii) study of potential constraints due to addition of new data set to fit

iii) perform high precision measurement of PDFs, strong coupling $\alpha_s(M_Z)$ and heavy quark masses m_c, m_b, m_t,

ABMP16 PDF ansatz

- PDFs parameterization at scale $\mu_0 = 3\mathrm{GeV}$ in scheme with $n_f = 3$

  Alekhin, Blümlein, S.M., Placakyte '17

  - ansatz for valence-/sea-quarks, gluon

$$
\begin{aligned}
xq_v(x,\mu_0^2) &= \frac{2\delta_{qu}+\delta_{qd}}{N_q^v} x^{a_q}(1-x)^{b_q} x^{P_{qv}(x)} \\
xq_s(x,\mu_0^2) &= x\bar{q}_s(x,\mu_0^2) = A_{qs}(1-x)^{b_{qs}} x^{a_{qs} P_{qs}(x)} \\
xg(x,\mu_0^2) &= A_g x^{a_g}(1-x)^{b_g} x^{a_g\, P_g(x)}
\end{aligned}
$$

  - strange quark is taken in charge-symmetric form
  - function $P_p(x)$

$$
P_p(x) = (1+\gamma_{-1,p}\ln x)\left(1+\gamma_{1,p}x+\gamma_{2,p}x^2+\gamma_{3,p}x^3\right) \,,
$$

  - 29 parameters in fit including $\alpha_s^{(n_f=3)}(\mu_0 = 3$ GeV), m_c, m_b and m_t
  - simultaneous fit of higher twist parameters (twist-4)
- Ansatz provides sufficient flexibility; no additional terms required to improve the quality of fit

Quality of fit

Statistical tests

- Goodness-of-fit estimator
  - χ^2 values compared to number of data points (typically a few thousand in global fit)

Covariance matrix

- Positive-definite covariance matrix
  - correlations for fit parameters of ABMP16 PDFs

	a_u	b_u	$\gamma_{1,u}$	$\gamma_{2,u}$	$\gamma_{3,u}$	a_d	b_d	$\gamma_{1,d}$	$\gamma_{2,d}$	$\gamma_{3,d}$
a_u	1.0	0.7617	0.9372	-0.5078	0.4839	0.4069	0.3591	0.4344	-0.3475	0.0001
b_u	0.7617	1.0	0.6124	-0.1533	-0.0346	0.3596	0.2958	0.3748	-0.2748	0.0001
$\gamma_{1,u}$	0.9372	0.6124	1.0	-0.7526	0.7154	0.2231	0.2441	0.2812	-0.2606	0.0001
$\gamma_{2,u}$	-0.5078	-0.1533	-0.7526	1.0	-0.9409	0.2779	0.2276	0.2266	-0.1860	0.0
$\gamma_{3,u}$	0.4839	-0.0346	0.7154	-0.9409	1.0	-0.1738	-0.1829	-0.1327	0.1488	0.0
a_d	0.4069	0.3596	0.2231	0.2779	-0.1738	1.0	0.7209	0.9697	-0.6529	0.0001
b_d	0.3591	0.2958	0.2441	0.2276	-0.1829	0.7209	1.0	0.7681	-0.9786	-0.0001
$\gamma_{1,d}$	0.4344	0.3748	0.2812	0.2266	-0.1327	0.9697	0.7681	1.0	-0.7454	0.0002
$\gamma_{2,d}$	-0.3475	-0.2748	-0.2606	-0.1860	0.1488	-0.6529	-0.9786	-0.7454	1.0	-0.0002
$\gamma_{3,d}$	0.0001	0.0001	0.0001	0.0	0.0	0.0001	-0.0001	0.0002	-0.0002	1.0
a_{us}	-0.0683	-0.0081	-0.2094	0.3881	-0.3206	0.2266	0.1502	0.2000	-0.1293	0.0
b_{us}	-0.3508	-0.3089	-0.3462	0.0906	-0.0537	-0.1045	-0.2000	-0.2241	0.2798	0.0
$\gamma_{-1,us}$	0.2296	0.1387	0.3367	-0.4043	0.3474	-0.1171	-0.1127	-0.0810	0.0767	0.0
$\gamma_{1,us}$	-0.4853	-0.4119	-0.3844	-0.0365	0.0064	-0.4380	-0.3592	-0.4957	0.3771	-0.0001
A_{us}	0.0506	0.0807	-0.0949	0.3198	-0.2560	0.2527	0.1648	0.2350	-0.1509	0.0
a_{ds}	-0.0759	-0.0443	-0.0951	0.0263	-0.0382	-0.2565	-0.2541	-0.2666	0.2380	0.0
b_{bs}	0.0452	-0.0197	0.0345	-0.0589	0.0683	-0.2084	0.0190	-0.1841	-0.0522	0.0
$\gamma_{1,ds}$	-0.0492	-0.0809	0.0101	-0.1791	0.1309	-0.5576	-0.2029	-0.4584	0.0946	0.0
A_{ds}	-0.1980	-0.1262	-0.2349	0.1526	-0.1428	-0.1113	-0.2167	-0.1739	0.2407	0.0
a_{ss}	-0.2034	-0.1285	-0.2362	0.2328	-0.2080	0.0960	0.1596	0.0661	-0.1054	0.0
b_{ss}	-0.1186	-0.0480	-0.1532	0.1549	-0.1536	0.0486	0.1508	0.0267	-0.1161	0.0
A_{ss}	-0.1013	-0.0411	-0.1458	0.1802	-0.1625	0.1216	0.1678	0.0924	-0.1196	0.0
a_g	0.0046	-0.0374	0.1109	-0.1934	0.1653	-0.0288	-0.0122	0.0053	0.0059	0.0
b_g	0.2662	0.3141	0.1579	-0.0050	-0.0207	0.0973	0.0870	0.0646	-0.0666	0.0
$\gamma_{1,g}$	0.2008	0.2274	0.0706	0.0876	-0.0835	0.0919	0.0574	0.0493	-0.0364	0.0
$\alpha_s^{(n_f=3)}(\mu_0)$	0.1083	-0.0607	0.0848	-0.0250	0.0765	0.0763	-0.0306	0.0725	0.0243	0.0
$m_c(m_c)$	-0.0006	0.0170	-0.0104	0.0206	-0.0201	-0.0123	-0.0161	-0.0114	0.0108	0.0
$m_b(m_b)$	0.0661	0.0554	0.0605	-0.0367	0.0287	-0.0116	0.0029	-0.0074	-0.0051	0.0
$m_t(m_t)$	-0.1339	-0.2170	-0.0816	0.0081	0.0250	-0.0616	-0.0813	-0.0491	0.0736	0.0

	a_{us}	b_{us}	$\gamma_{-1,us}$	$\gamma_{1,us}$	A_{us}	a_{ds}	b_{bs}	$\gamma_{1,ds}$	A_{ds}	a_{ss}
a_u	-0.0683	-0.3508	0.2296	-0.4853	0.0506	-0.0759	0.0452	-0.0492	-0.1980	-0.2034
b_u	-0.0081	-0.3089	0.1387	-0.4119	0.0807	-0.0443	-0.0197	-0.0809	-0.1262	-0.1285
$\gamma_{1,u}$	-0.2094	-0.3462	0.3367	-0.3844	-0.0949	-0.0951	0.0345	0.0101	-0.2349	-0.2362
$\gamma_{2,u}$	0.3881	0.0906	-0.4043	-0.0365	0.3198	0.0263	-0.0589	-0.1791	0.1526	0.2328
$\gamma_{3,u}$	-0.3206	-0.0537	0.3474	0.0064	-0.2560	-0.0382	0.0683	0.1309	-0.1428	-0.2080
a_d	0.2266	-0.1045	-0.1171	-0.4380	0.2527	-0.2565	-0.2084	-0.5576	-0.1113	0.0960
b_d	0.1502	-0.2000	-0.1127	-0.3592	0.1648	-0.2541	0.0190	-0.2029	-0.2167	0.1596
$\gamma_{1,d}$	0.2000	-0.2241	-0.0810	-0.4957	0.2350	-0.2666	-0.1841	-0.4584	-0.1739	0.0661
$\gamma_{2,d}$	-0.1293	0.2798	0.0767	0.3771	-0.1509	0.2380	-0.0522	0.0946	0.2407	-0.1054
$\gamma_{3,d}$	0.0	0.0	0.0	-0.0001	0.0	0.0	0.0	0.0	0.0	0.0
a_{us}	1.0	-0.3156	-0.8947	-0.5310	0.9719	0.2849	0.0241	-0.0470	0.2983	0.4131
b_{us}	-0.3156	1.0	0.1372	0.8258	-0.3995	0.0467	-0.0221	-0.1190	0.1856	0.0291
$\gamma_{-1,us}$	-0.8947	0.1372	1.0	0.2611	-0.7829	-0.1695	0.0156	0.0501	-0.2117	-0.7191
$\gamma_{1,us}$	-0.5310	0.8258	0.2611	1.0	-0.6479	0.0086	0.0076	0.1460	0.0781	-0.0010
A_{us}	0.9719	-0.3995	-0.7829	-0.6479	1.0	0.2983	0.0515	-0.0404	0.3055	0.2811
a_{ds}	0.2849	0.0467	-0.1695	0.0086	0.2983	1.0	-0.1608	0.0719	0.9152	-0.2941
b_{bs}	0.0241	-0.0221	0.0156	0.0076	0.0515	-0.1608	1.0	0.7834	-0.3022	-0.0390
$\gamma_{1,ds}$	-0.0470	-0.1190	0.0501	0.1460	-0.0404	0.0719	0.7834	1.0	-0.1838	-0.1373
A_{ds}	0.2983	0.1856	-0.2117	0.0781	0.3055	0.9152	-0.3022	-0.1838	1.0	-0.1833
a_{ss}	0.4131	0.0291	-0.7191	-0.0010	0.2811	-0.2941	-0.0390	-0.1373	-0.1833	1.0
b_{ss}	0.2197	0.0643	-0.4479	0.1286	0.1193	-0.1579	-0.0260	0.0169	-0.0896	0.6522
A_{ss}	0.3627	0.0261	-0.6319	0.0102	0.2412	-0.2688	-0.0180	-0.0960	-0.1797	0.9280
a_g	-0.2570	0.0001	0.2196	0.0039	-0.2493	-0.2190	-0.0454	-0.1031	-0.2571	0.0626
b_g	-0.1419	0.1266	0.0694	0.2648	-0.1715	-0.0515	0.0917	0.2130	-0.0469	-0.0092
$\gamma_{1,g}$	-0.0241	0.0332	-0.0226	0.1296	-0.0489	-0.0137	0.0503	0.1409	0.0022	-0.0279
$\alpha_s^{(n_f=3)}(\mu_0)$	0.0954	-0.2866	-0.0341	-0.3493	0.1110	-0.0604	-0.1265	-0.1811	-0.1330	-0.0841
$m_c(m_c)$	0.0704	-0.0093	-0.0033	-0.0462	0.1182	0.0849	0.0547	0.0413	0.1193	-0.0728
$m_b(m_b)$	-0.0183	-0.0132	0.0044	0.0209	-0.0298	-0.0006	0.0332	0.0695	-0.0432	-0.0159
$m_t(m_t)$	0.0641	-0.1841	-0.0408	-0.2635	0.0755	-0.0573	-0.1067	-0.2003	-0.0869	0.0169

	b_{ss}	A_{ss}	a_g	b_g	$\gamma_{1,g}$	$\alpha_s^{(n_f=3)}(\mu_0)$	$m_c(m_c)$	$m_b(m_b)$	$m_t(m_t)$
a_u	-0.1186	-0.1013	0.0046	0.2662	0.2008	0.1083	-0.0006	0.0661	-0.1339
b_u	-0.0480	-0.0411	-0.0374	0.3141	0.2274	-0.0607	0.0170	0.0554	-0.2170
$\gamma_{1,u}$	-0.1532	-0.1458	0.1109	0.1579	0.0706	0.0848	-0.0104	0.0605	-0.0816
$\gamma_{2,u}$	0.1549	0.1802	-0.1934	-0.0050	0.0876	-0.0250	0.0206	-0.0367	0.0081
$\gamma_{3,u}$	-0.1536	-0.1625	0.1653	-0.0207	-0.0835	0.0765	-0.0201	0.0287	0.0250
a_d	0.0486	0.1216	-0.0288	0.0973	0.0919	0.0763	-0.0123	-0.0116	-0.0616
b_d	0.1508	0.1678	-0.0122	0.0870	0.0574	-0.0306	-0.0161	0.0029	-0.0813
$\gamma_{1,d}$	0.0267	0.0924	0.0053	0.0646	0.0493	0.0725	-0.0114	-0.0074	-0.0491
$\gamma_{2,d}$	-0.1161	-0.1196	0.0059	-0.0666	-0.0364	0.0243	0.0108	-0.0051	0.0736
$\gamma_{3,d}$	0.0	0.0	0.0	0.0	0.0	0.0	0.0	0.0	0.0
a_{us}	0.2197	0.3627	-0.2570	-0.1419	-0.0241	0.0954	0.0704	-0.0183	0.0641
b_{us}	0.0643	0.0261	0.0001	0.1266	0.0332	-0.2866	-0.0093	-0.0132	-0.1841
$\gamma_{-1,us}$	-0.4479	-0.6319	0.2197	0.0694	-0.0226	-0.0341	-0.0034	0.0044	-0.0408
$\gamma_{1,us}$	0.1286	0.0102	0.0039	0.2648	0.1296	-0.3493	-0.0462	0.0209	-0.2635
A_{us}	0.1193	0.2412	-0.2493	-0.1715	-0.0489	0.1110	0.1182	-0.0298	0.0755
a_{ds}	-0.1579	-0.2688	-0.2190	-0.0515	-0.0137	-0.0604	0.0849	-0.0006	-0.0573
b_{bs}	-0.0260	-0.0180	-0.0454	0.0917	0.0503	-0.1265	0.0547	0.0332	-0.1067
$\gamma_{1,ds}$	0.0169	-0.0960	-0.1031	0.2130	0.1409	-0.1811	0.0413	0.0695	-0.2003
A_{ds}	-0.0896	-0.1797	-0.2571	-0.0469	0.0022	-0.1330	0.1193	-0.0432	-0.0869
a_{ss}	0.6522	0.9280	0.0626	-0.0092	-0.0279	-0.0841	-0.0728	-0.0159	0.0169
b_{ss}	1.0	0.6427	-0.0179	0.1967	0.1164	-0.2390	-0.0965	0.0169	-0.1675
A_{ss}	0.6427	1.0	-0.0211	0.1403	0.0997	-0.1385	0.0216	0.0072	-0.1109
a_g	-0.0179	-0.0211	1.0	-0.5279	-0.8046	0.1838	-0.2829	0.0076	0.3310
b_g	0.1967	0.1403	-0.5279	1.0	0.8837	-0.5124	0.1438	0.1255	-0.7275
$\gamma_{1,g}$	0.1164	0.0997	-0.8046	0.8837	1.0	-0.2511	0.1829	0.0814	-0.5180
$\alpha_s^{(n_f=3)}(\mu_0)$	-0.2390	-0.1385	0.1838	-0.5124	-0.2511	1.0	-0.1048	0.0423	0.6924
$m_c(m_c)$	-0.0965	0.0216	-0.2829	0.1438	0.1829	-0.1048	1.0	0.0328	-0.1577
$m_b(m_b)$	0.0169	0.0072	0.0076	0.1255	0.0814	0.0423	0.0328	1.0	-0.0900
$m_t(m_t)$	-0.1675	-0.1109	0.3310	-0.7275	-0.5180	0.6924	-0.1577	-0.0900	1.0

Results for parton distributions

- PDFs with 1σ uncertainty bands; compare ABMP16, CT14, MMHT14 NNPDF3.0
- Gluon $g(x)$

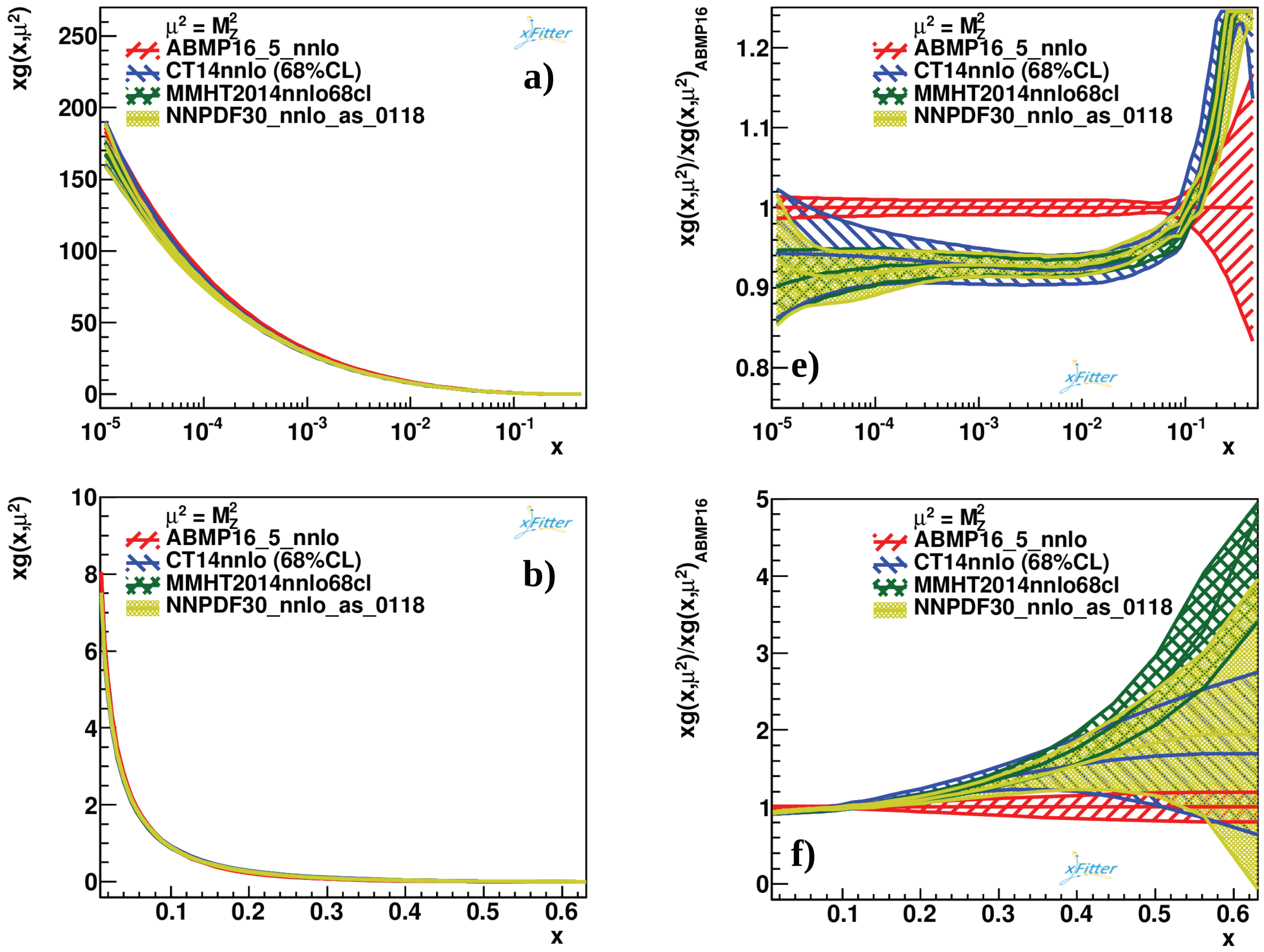

Top-quark hadro-production cross section

- Cross section for $t\bar{t}$-production with parametric dependence

$$\sigma_{pp\to X} \quad = \quad \sum_{ij} f_i(\mu^2) \otimes f_j(\mu^2) \otimes \underbrace{\hat{\sigma}_{ij\to X}\left(\alpha_s(\mu^2), Q^2, \mu^2, m_X^2\right)}$$

$$= \hat{\sigma}^{(0)}_{ij\to X} + \alpha_s\, \hat{\sigma}^{(1)}_{ij\to X} + \alpha_s^2\, \hat{\sigma}^{(2)}_{ij\to X} + \dots$$

  - PDFs f_i, strong coupling α_s, masses m_X
- Correlation of PDFs, $\alpha_s(M_Z)$ and m_t in global fit
  - effective parton $\langle x \rangle \sim 2m_t/\sqrt{s} \sim 2.5 \dots 5 \cdot 10^{-2}$

Top-quark mass determination

- Choice of renormalization scheme for treatment of heavy quarks
  - heavy quark mass in on-shell scheme $m_t^{\rm pole}$
  - running quark mass in $\overline{\rm MS}$-scheme $m_t(\mu)$
- Intrinsic limitation of sensitivity in total cross section

$$\left| \frac{\Delta\sigma_{t\bar{t}}}{\sigma_{t\bar{t}}} \right| \simeq 5 \times \left| \frac{\Delta m_t}{m_t} \right|$$

Data on top-quark cross sections

experiment	decay channel	dataset	luminosity	$\sqrt{s}$	ref.
ATLAS & CMS	combined	2011	5 fb^{-1}	7 TeV	2205.13830
ATLAS & CMS	combined	2012	20 fb^{-1}	8 TeV	2205.13830
ATLAS	dileptonic, semileptonic	2011	257 pb^{-1}	5.02 TeV	2207.01354
CMS	dileptonic	2011	302 pb^{-1}	5.02 TeV	2112.09114
ATLAS	dileptonic	2015-2018	140 fb^{-1}	13 TeV	2303.15340
ATLAS	semileptonic	2015-2018	139 fb^{-1}	13 TeV	2006.13076
CMS	dileptonic	2016	35.9 fb^{-1}	13 TeV	1812.10505
CMS	semileptonic	2016-2018	137 fb^{-1}	13 TeV	2108.02803
ATLAS	dileptonic	2022	11.3 fb^{-1}	13.6 TeV	ATLAS-CONF-2023-006
CMS	dileptonic, semileptonic	2022	1.21 fb^{-1}	13.6 TeV	2303.10680

Experiment	decay channel	dataset	luminosity	$\sqrt{s}$	observable(s)	n	ref.
CMS	semileptonic	2016–2018	137 fb^{-1}	13 TeV	$M(t\bar{t})$, $\lvert y(t\bar{t})\rvert$	34	2108.02803
CMS	dileptonic	2016	35.9 fb^{-1}	13 TeV	$M(t\bar{t})$, $\lvert y(t\bar{t})\rvert$	15	1904.05237
ATLAS	semileptonic	2015–2016	36 fb^{-1}	13 TeV	$M(t\bar{t})$, $\lvert y(t\bar{t})\rvert$	19	1908.07305
ATLAS	all-hadronic	2015–2016	36.1 fb^{-1}	13 TeV	$M(t\bar{t})$, $\lvert y(t\bar{t})\rvert$	10	2006.09274
CMS	dileptonic	2012	19.7 fb^{-1}	8 TeV	$M(t\bar{t})$, $\lvert y(t\bar{t})\rvert$	15	1703.01630
ATLAS	semileptonic	2012	20.3 fb^{-1}	8 TeV	$M(t\bar{t})$	6	1511.04716
ATLAS	dileptonic	2012	20.2 fb^{-1}	8 TeV	$M(t\bar{t})$	5	1607.07281
ATLAS	dileptonic	2011	4.6 fb^{-1}	7 TeV	$M(t\bar{t})$	4	1607.07281
ATLAS	semileptonic	2011	4.6 fb^{-1}	7 TeV	$M(t\bar{t})$	4	1407.0371

- Measurements of top-quark hadro-production ATLAS, CMS
  - total inclusive $t\bar{t} + X$ cross sections ($NDP = 10$)
  - differential $t\bar{t} + X$ cross sections in $M(t\bar{t})$, $y(t\bar{t})$ ($NDP = 112$)

Fit quality

Data set	n	ABMP16	CT18	MSHT20	NNPDF4.0
CMS 13 TeV semileptonic 2108.02803	34	19(20)	29(176)	38(132)	55(90)
CMS 13 TeV dileptonic 1904.05237	15	15(15)	23(38)	27(34)	23(23)
ATLAS13 TeV semileptonic 1908.07305	19	11(15)	12(17)	11(13)	12(12)
ATLAS 13 TeV all-hadronic 2006.09274	10	11(11)	16(19)	16(17)	14(14)
CMS 8 TeV dileptonic 1703.01630	15	11(15)	11(12)	11(12)	12(12)
ATLAS 8 TeV semileptonic 1511.04716	6	10(12)	4(4)	4(4)	5(5)
ATLAS 7 TeV dileptonic 1607.07281	4	2(3)	1.9(1.9)	1.6(1.6)	1.1(1.1)
ATLAS 8 TeV dileptonic 1607.07281	5	0.2(0.2)	0.4(0.5)	0.4(0.4)	0.2(0.2)
ATLAS 7 TeV semileptonic 1407.0371	4	0.9(1.0)	5(6)	6(6)	3(3)
$\sigma(t\bar{t})$ all ATLAS + CMS incl. data	10	11(26)	16(61)	16(43)	11(12)
Total	122	101(117)	115(337)	113(262)	129(172)

- Global and partial χ^2 values for each data set
  - number of data points (n) obtained in $m_t^{\rm pole}$ extraction
  - different PDF sets ABMP16, CT18, MHST20, NNPDF4.0
- Additional χ^2 values in parentheses omit PDF uncertainties

Top-quark data in ABMP fit

ABMPtt PDF fit

Alekhin, Garzelli, S.M., Zenaiev '24

- New PDF fit with differential LHC top-quark data in ABMP framework
  - simultenous determination of proton PDFs, strong coupling, and heavy-quark masses at NNLO QCD
  - strong coupling $\alpha_s(M_Z) = 0.1150 \pm 0.0009$
  - top-quark $\overline{\text{MS}}$ mass $m_t(m) = 160.6 \pm 0.6$ GeV
  - pole mass $m_t(m) = 170.2 \pm 0.7$ GeV

Upshot

- Good compatibilty of PDFs from ABMP16tt and ABMP16
- Confirmation of gluon PDF in range $x \simeq 10^{-2}$ with reduced uncertainties compared to ABMP16
- PDFs sets available in LHAPDF for fixed number of flavors, $n_f = 3, 4, 5$
  ABMPtt_3_nnlo (0+29)
  ABMPtt_4_nnlo (0+29)
  ABMPtt_5_nnlo (0+29)

ABMPtt PDFs (I)

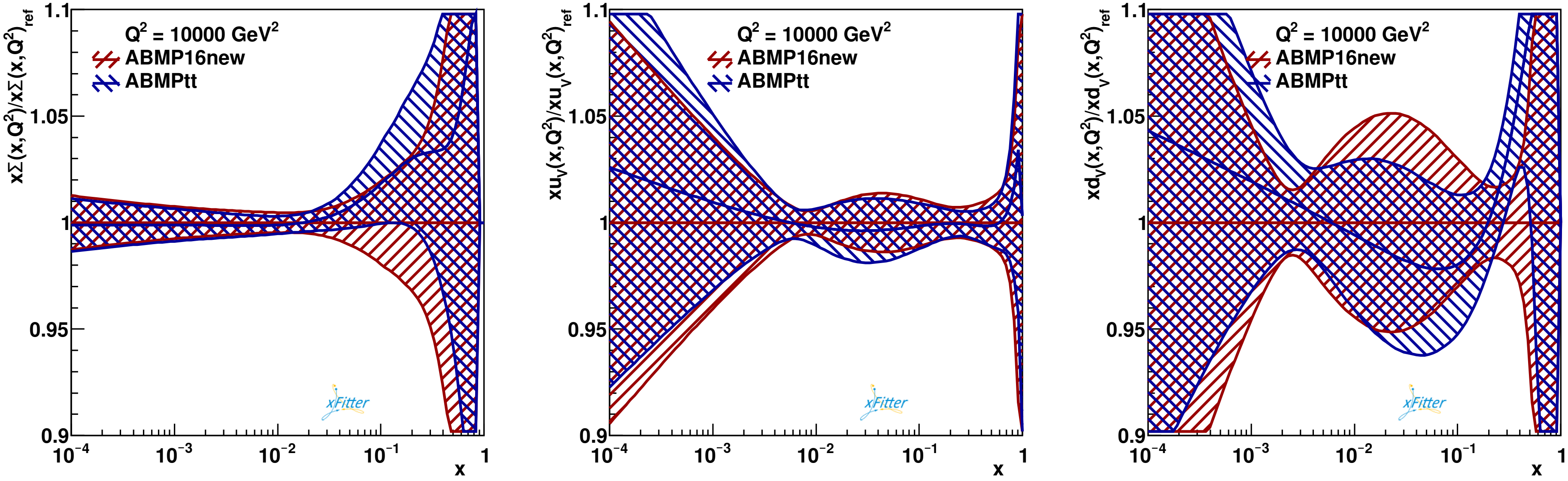

- Ratio of PDFs (sea-quark, valence up- and down-quark) at scale $Q = 100$ GeV for $n_f = 5$
  - fit ABMP16tt vs. ABMP16

ABMPtt PDFs (II)

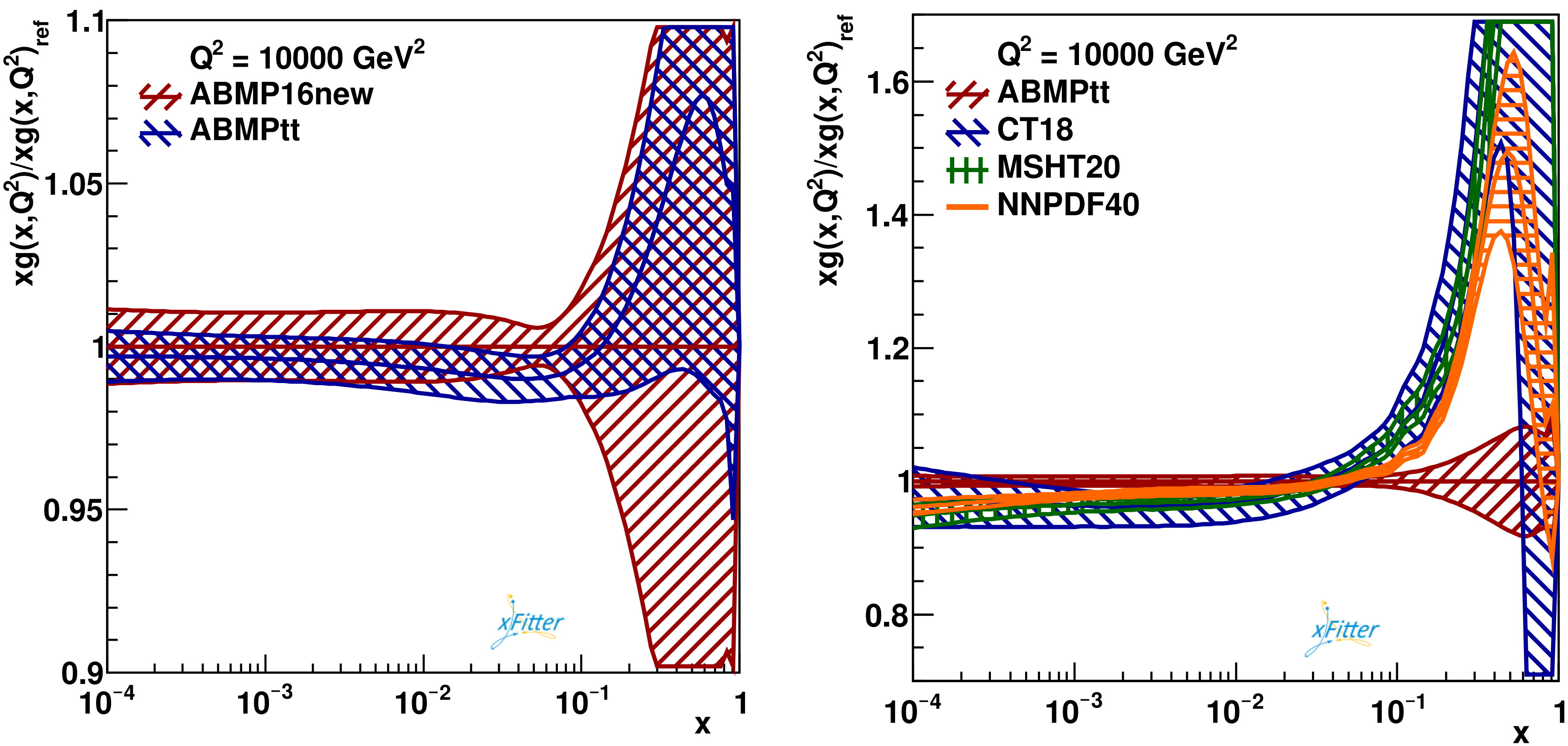

- Ratio of gluon PDF at scale $Q = 100$ GeV for $n_f = 5$
  - fit ABMP16tt vs. ABMP16
  - comparison to different PDF sets CT18, MHST20, NNPDF4.0

Summary (part IV)

Deep structure of proton

- Parton evolution
  - factorization induces evolution equations via renormalization group
  - parton distribution function from global fits to data
- Parton luminosity for hadron colliders
  - kinematics plane in x and Q^2 for present and future colliders
- Precision studies of hadron structure
  - dedicated analysis of experimental data
  - correlations of PDFs with $\alpha_s(M_Z)$ and top-quark mass extraction
- New ABMPtt PDF fit
  - Confirmation of gluon PDF in x-range relevant for Higgs production at LHC